Journal of Mining and Geology Vol. 60(1) 2024. pp. 57 - 71 0022-2763

www.nmgs-journal.org

Facies Analysis, Mineralogy, and Geochemistry of thePaleocene Ewekoro Formation, Dahomey Basin, Southwestern Nigeria: *Implications for Palaeodepositional Environments*

Bankole, S.I.[*], Opatola, A.O., Onah, C.E., Ogunmodede, O.P., Abiodun, A.S. and Bashorun, D.A.
Department of Geosciences, University of Lagos, Lagos, Nigeria.
Corresponding E-mail: sbankole@unilag.edu.ng

Abstract
The extensive limestone (carbonate) deposits of the Paleocene Ewekoro Formation, were petrographically, mineralogically and geochemically investigated for depositional environmental interpretation. Thin section of selected samples were prepared for petrographical analysis. Mineralogical and geochemical analyses, using X-ray diffraction analysis (XRD), Inductively Coupled Plasma Optical Emission Spectroscopy (ICP- OES), and Inductively Coupled Plasma Mass Spectrometry (ICP-MS) were conducted on twenty limestone samples. Two microfacies including packstone and wackestone were identified on the basis component composition. The microfacies reflected fossils of organisms characteristic of low to moderate energy, shallow marine environments. Calcite dominates the mineral constituent of the limestone, with accessory minerals such as quartz, muscovite, and albite occurring is moderate amounts. The Post-Archean Australian Shale (PAAS) normalized REE+Y of the limestones displays relatively uniform patterns (enriched LREE, positive Ce anomaly, and High Y/Ho ratio) across the different lithologies. The enrichment of LREE and depletion of HREE as reflected by the (La/Yb)sn. (Dy/Yb)sn and (Nd/Yb)sn ratios suggest a non-seawater like characteristics, probably a brackish water environment. Elemental ratios of Eu/Eu*. La/Co, Th/Co, Th/Cr, and Cr/Th suggest terrigenous contributions derived probably from intermediate to felsic rocks. The geochemical proxies, including the V/(V+Ni), V/Ni, V/Mo, Th/U ratios, Ce anomaly, and Mn* indicate that the limestones were deposited in a shallow marine environment under a fluctuating oxidizing to reducing conditions.

Keywords: *Ewekoro, Limestone, Packstone, Wackestone, Facies.*

Introduction

Extensive limestone deposits abounds in the Nigerian sedimentary basins including but not limited to the Sokoto, Anambra and Dahomey Basins. This essential industrial mineral which finds its use in the construction, agricultural and many other industries covers close to fifteen percent of the world's sedimentary basins (Wilson, 1975). Shallow, warm marine environments which are habitats for carbonate frame building organisms including brachiopods, ammonites, gastropods, foraminifera, ostracod and many other macro- and micro shelly organisms favour limestone accumulation. Limestone successions are reported in environmental settings such as continental basin margins (Wilson, 1975), oceanic floors above carbonate compensation depths (CCD) and some inland basins (Kerr, 2014; Zhang et al., 2014; Liu et al., 1988; Nath et al., 1997; Alonso-Zarza, 2003). Limestone is primarily composed of $CaCO_3$, however, it also contains a variety of major, trace and rare earth elements obtained through metalliferous and terrigenous particulates and scavenging from seawater (Bertram and Elderfield, 1993; Siby et al., 2008).

The Paleocene limestone deposits of the Ewekoro Formation is an extensive deposit which straddles the eastern sector of the Dahomey Basin, located in Western Nigeria. The deposit has been subject of diverse study (Bankole, et al., 2021; Akaegbobi and Ogungbesan, 2016; Adekeye and Akande, 2006).

The inclusion of rare earth elements (REE) in carbonate rocks provides important information on depositional conditions such as oceanic paleo-redox conditions (German and Elderfield, 1990; Murray et al., 1991) and diagenetic processes (Madhavaraju and Ramasamy, 1999; Armstrong-Altrin et al., 2003). REE in sediments do not easily migrate. Hence, the REE signatures in carbonates are widely used to trace the geochemical properties of the surrounding fluids (such as seawater and pore water) and environmental conditions during primary carbonate deposition.

The present study is aimed at using facies analysis and component association, sedimentological characteristics, mineralogy, and geochemistry to decipher the prevailing depositional conditions during the accumulation of the Ewekoro Limestones.

Geological Setting and Stratigraphy of the Study Area

The study area is located in the eastern Dahomey Basin, southwestern Nigeria (Fig. 1). It is an extensive sedimentary basin formed from the amalgamation of inland/coastal/offshore basins that extends from southeastern Ghana through Togo and the Republic of Benin to southwestern Nigeria. It is separated from the Niger Delta by a subsurface basement ridge referred to as the Okitipupa Ridge.

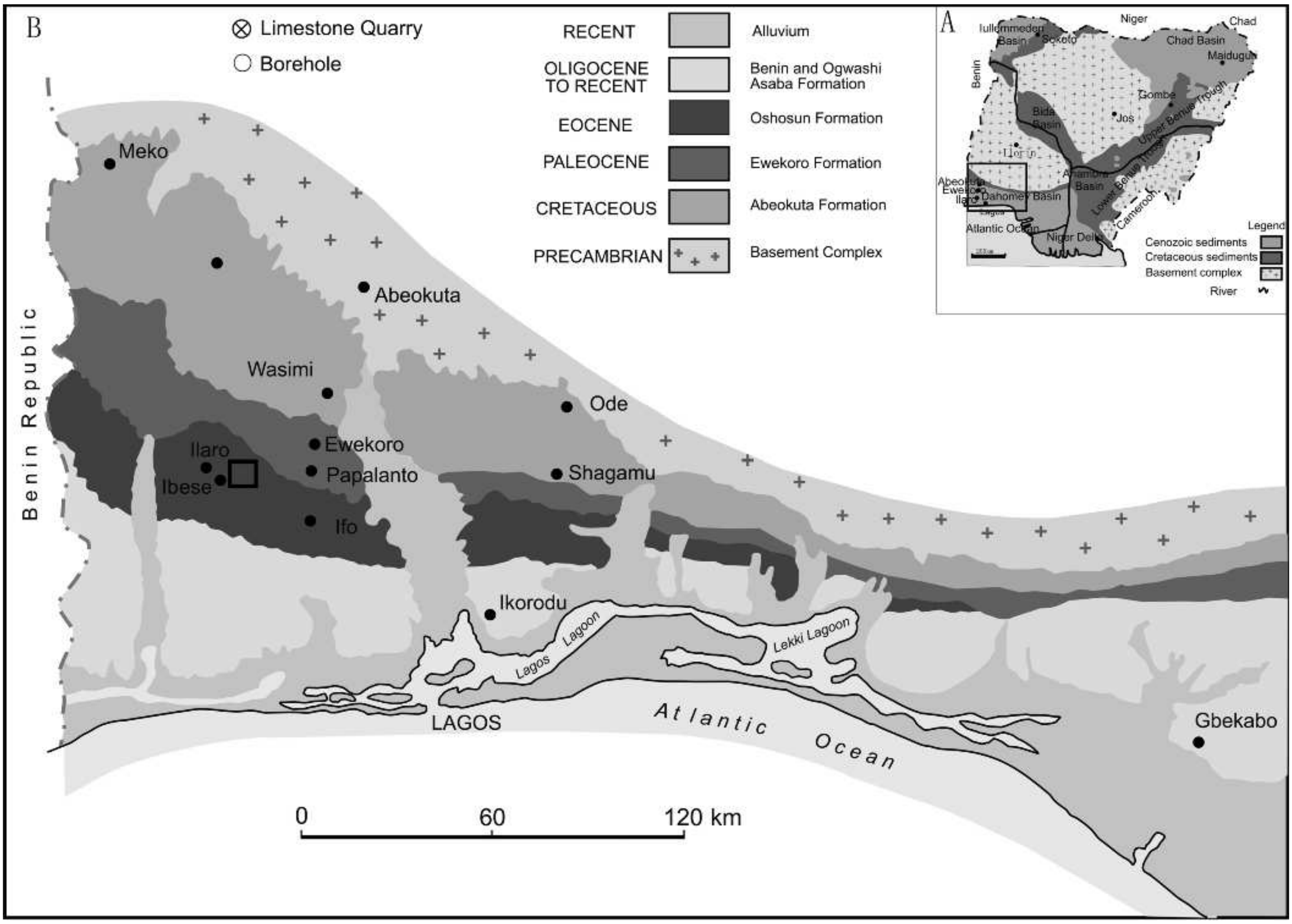

Fig. 1: Geological map of the eastern Dahomey Basin. Inset; Geological sketch map of Nigeria. The rectangle shows the study area. (The Eastern Dahomey Basin Map is modified after Bankole *et al.*, 2006).

Early researchers on the evolution and stratigraphy of the eastern Dahomey Basin include Jones and Hockey, 1964; Reyment 1965; Ogbe, 1972; Omatsola and Adegoke, 1981, and Billman, 1976 among others. The stratigraphy of the Basin (Fig. 2) is divided into the Cretaceous sediments of the Abeokuta Group, composed of the Ise, Afowo, and Araromi Formations, and the Tertiary sediments of the Ewekoro, Ososun, and Ilaro Formations. The present study focuses on the Ewekoro Formation, which is an extensive limestone deposit resulting from the shallow warm marine environment during the Paleocene. The Ewekoro Formation is highly fossiliferous, comprising coralline algae, gastropods, pelecypods, echinoid fragments, and other skeletal debris.

The study area is a massive limestone quarry. The deposit, in the quarry is divided into two sectors; the low grade and high grade occupying the northeastern and the southwestern sectors of the quarry respectively (Fig. 3). The low-grade area is characterized by thin overburden, mainly clay, grading, to lateritic soil. In the contrary, the high-grade area is covered by massive grey to dark grey shale overburden shielding the underlying limestone from meteoric water percolation.

Materials and Methods

Four of the six sections logged durig the field investigation are represent in figure 4. From the logged sections, a total of twenty two samples collected for analyses. The analyses include thin sectioning, X-Ray diffractometer (XRD) and combined ICP-MS and ICP-OES for component identification, mineral

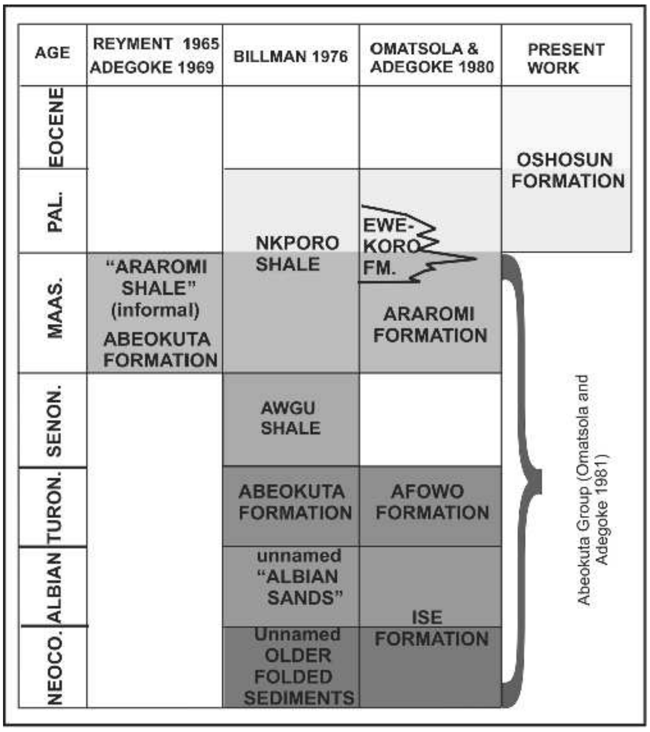

Fig. 2: Generalized Age and stratigraphic setting of the Dahomey Basin (Bankole et al., 2006)

identification and elemental concentration respectively. Thin sectioning was carried at the rock laboratory of the Department of Geology, Kwara State University, Nigeria. Petrographical scanning for facies analysis and component identification was conducted at the sedimentological laboratory of the Department of Geosciences, University of Lagos. XRD analysis for mineral identification was conducted at the NGSA laboratory, Kaduna. The geochemical analyses were carried out at the SGS Laboratory, Randfonten, South Africa.

Mineralogical Analysis

Ten limestone samples from the twenty samples collected were selected for XRD analysis. One to two grams of the pulverized sample was weighed into the sample holder, and with the use of a glass slide, the sample was compacted to give an even surface area. The sample holder was then placed in the XRD multi-sample holders' chamber, and the machine calibrated to begin the analysis. Thereafter, the analyzed sample(s) were automatically saved into a directory folder, which is further uploaded to STUDIO SMART LAB II in

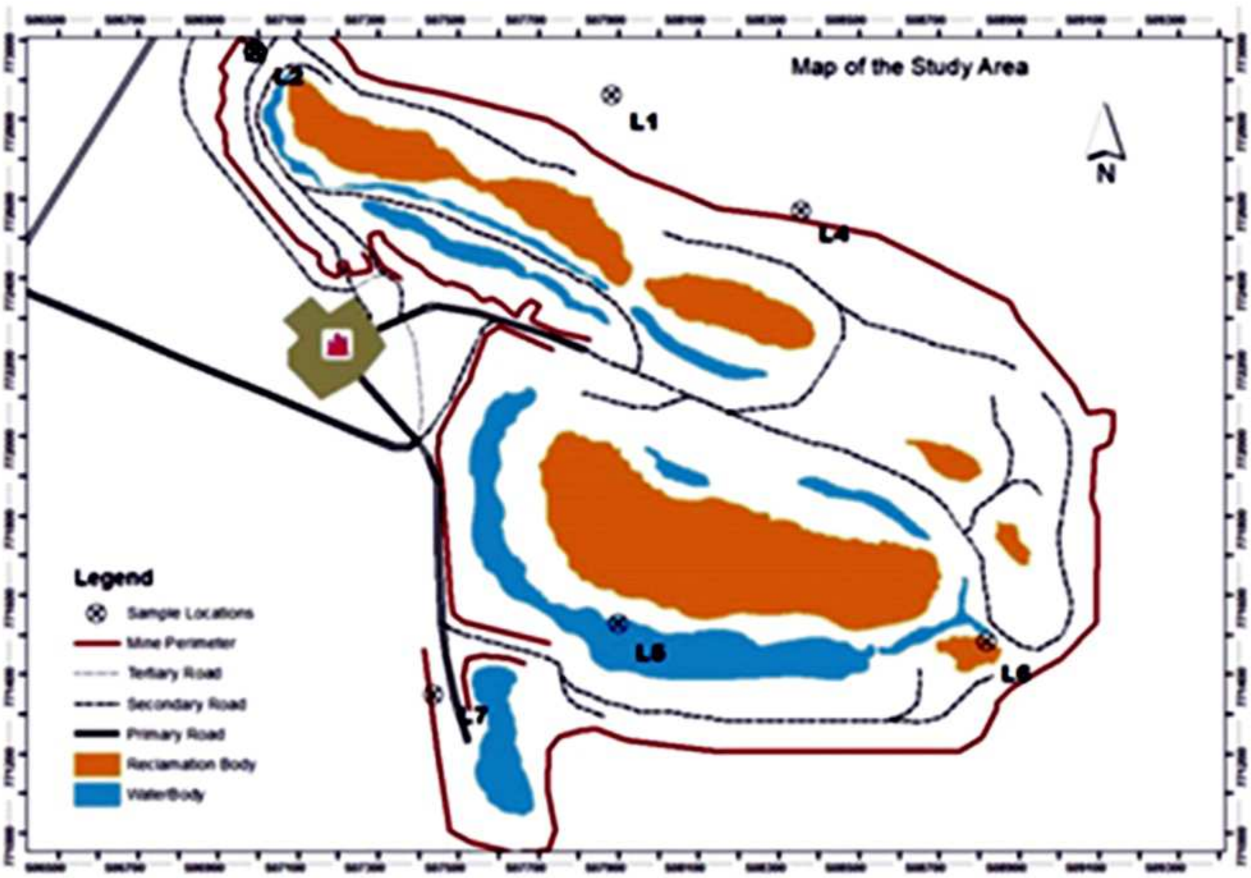

Fig. 3: Map of the South-Western Mine (SWM) in the Ibese quarry and sample locations

conjunction with ICDD PDF-4 to perform an automatic/manual search-match. The results of the analysis are then generated and either saved for reference purposes or printed out.

Geochemical Analysis

After pulverization, 0.10 g of the sample was weighed into a crucible with Sodium Oxide and Sodium Hydroxide (Na_2O + NaOH) added to the sample, mixed, and fused. After the fusion, the sample was leached, acidified, and made up to volume. The solution obtained was then analyzed using ICP-OES and ICP-MS. To ensure accuracy and precision, a minimum of one Reagent Blank and Certified/In-house Reference Material and one replicate was used with the batch of samples. After the analysis was completed, the resulting data was fed to the laboratory information management system with a secure audit trail.

Results and Interpretation

Lithological Results

The Ewekoro Formation, as sampled in the six studied sections consists of limestones that are distinctively of two grades: the low-grade and high-grade. This distinction is made on the basis of the percentage concentration of $CaCO_3$, and alumina content of the limestone. The percentage concentration of $CaCO_3$ in the high-grade limestones is greater than 50% and a low percentage concentration of alumina. Conversely, the percentage concentration of $CaCO_3$ in the low-grade limestone is less than 50% and a significant percentage concentration of alumina. Field relations show that the low-grade limestones are devoid of thick shale overburden, majorly overlain by thin clay and lateritic soil. These allowed percolation of meteoric water, resulting in extensive weathering, giving the limestone a yellowish coloration. Prevalence of vugs, filled with organic matter, characterises the low grade limestone. The vugs develop in response to dissolution of limestone by the percolating meteoric water. On the contrary, the high-grade limestone is overlain by thick shale overburden, shielding the deposit from meteoric water percolation, resulting in highly lithified rock with greyish to whitish colour. Though the presence of vugs could be observed in the high grade limestone, but only common at the upper section. The limestone deposit in the investigated area dips in northwest-southeast direction. The low-grade limestones are located in the northwestern sector of the study, with the high-grade counterpart occupying the southeastern portion.

The Ewekoro Limestone is highly fossiliferous, with highest concentration of fossils in the uppermost section prior to the deposition of the relatively thinly bedded (10 cm to 1.5 m) glauconitic sand which directly overly the limestone (Figs. 4A-D).

Laboratory Analytical Results

Petrography: The component of the studied limestone includes bioclasts, micrites, and sparry calcite. The bioclasts comprise of skeletal grains including, foraminifera, gastropods, brachiopods, bivalves, ostracodes, echinoderms, and green algae, while the non-skeletal grains consist of ooids, oncoids peloids (Figs. 5 and 6). Based on the classification scheme of Dunham (1962), two microfacies are identified.

Carbonate Classification

Packstone: Bioclastic Packstone: It is characterized by the presence of skeletal grains, including bivalves, echinoids, brachiopod spines, and algae and an abundance of non-skeletal ooids. The outer layer of the ooid casts were well preserved with thin micritic coating, however the nuclei had been replaced with sparry calcite. (Figs. 5A-C).

Gastropod-Ostracod Packstone: casts of skeletal grains including gastropods, fragmented and whole ostracodes, and bivalves. The high inward spire was the characteristic feature used to identify the gastropod shell. The gastropod shells have thickened, ornamented calcitic rims with small cavities. The original aragonite material of the shell was replaced with sparry calcite, and the cavities are filled with micrite. The gastropod grains are surrounded by grains of foraminifera, brachiopods, and bivalves (Figs. 5D - F).

Bioclastic Packstone: It is characterized by the presence of skeletal grains, including brachiopod shell, fragmented ostracod, orbitolinid foraminifera, biserial foraminifera, bryozoan, and phylloid algal Most of which have had their original mold replaced by sparry calcite with negligible micrite infillings (Fig. 5G-L).

Wackstone: Skeletal Wackestone: This microfacies consists of skeletal grains, including, crinoids, brachiopod spines, brachiopod shells, and differentiated tests and globigerina floating on microsparite cement (Figs. 6A-F).

Gastropod-Foraminifera Wackestone: Gastropod shells with their internal mold replaced with microspar

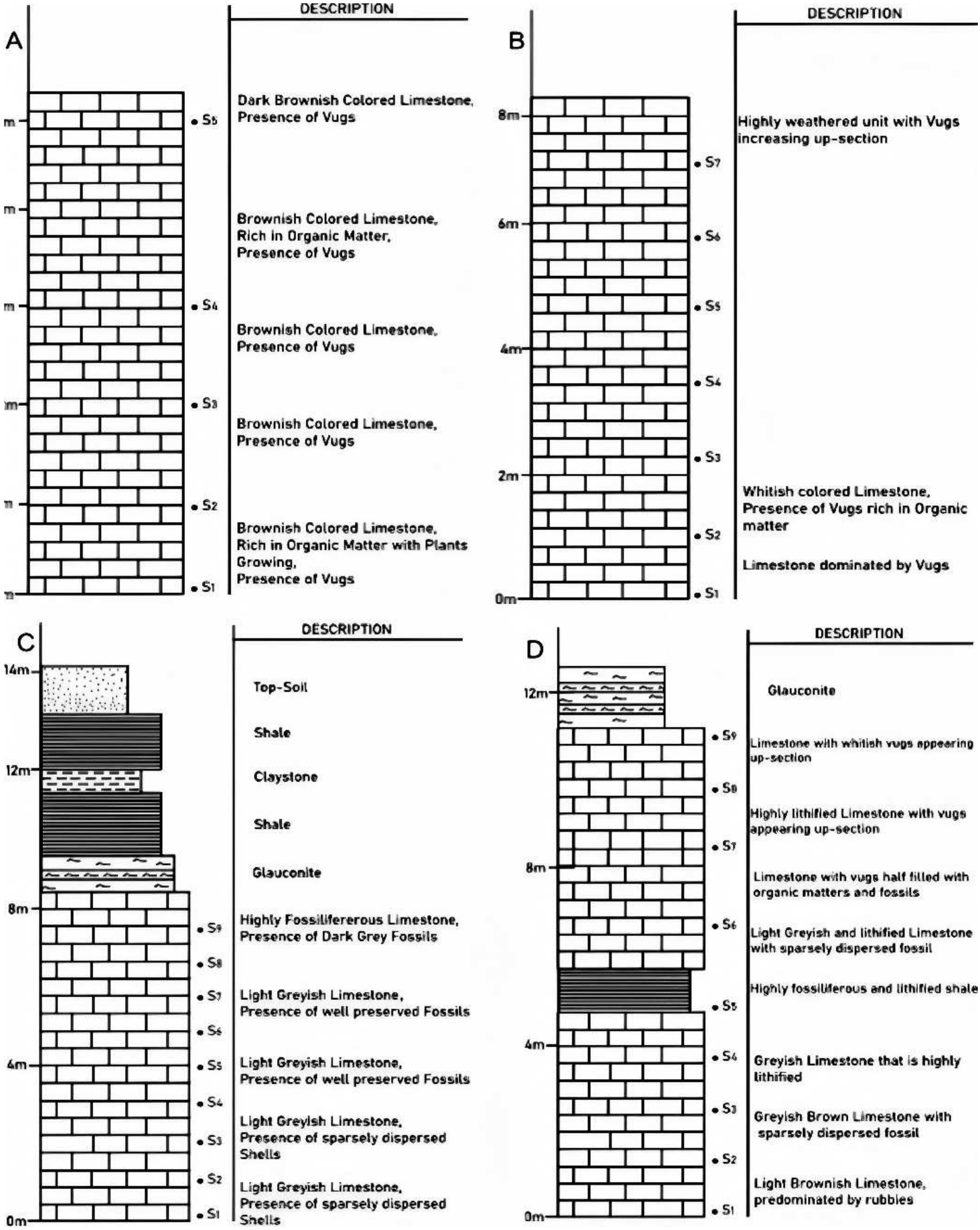

Fig. 4: (A-D) Logged sections of the studied Paleocene Ewekoro Limestone samples. ***A-B*** Lithologic section of low-grade limestones in the study area. ***C-D*** Lithologic section of high-grade limestones in the study area

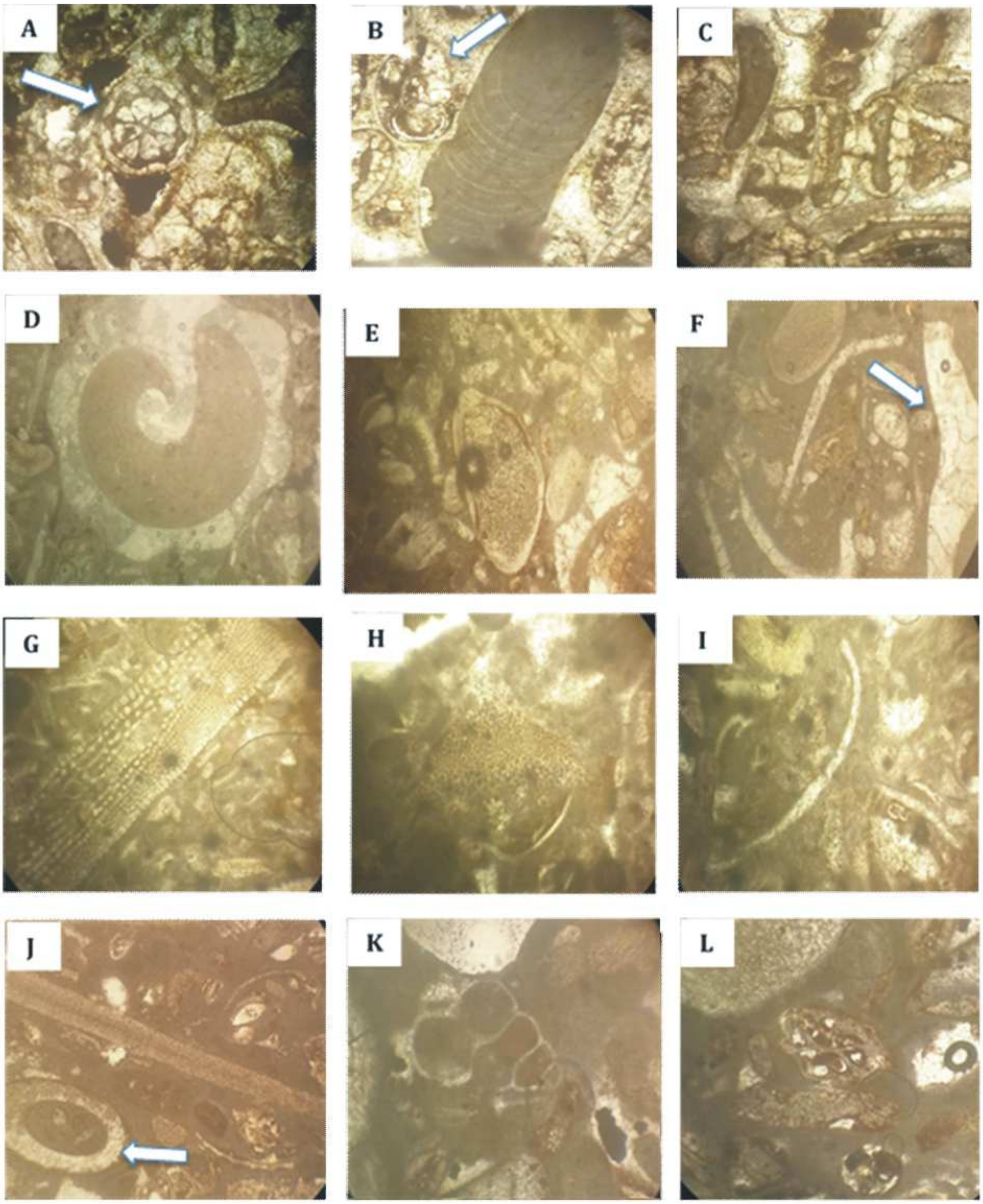

Fig. 5: A. (Arrow) An echinoderm spine with a distinct radial septa and negligible micrite infillings, surrounded by bioclasts and ooids. **B.** red algae with segments consisting of nearly equal cells and a cortex composed of tiny cells. The reticular appearance is due to micrite walls separating the small cell surrounded by ooids (Arrow)with nucleus replaced by sparry calcite. **C.** fragments of micritized bivalve shells embedded in a coating of calcite. **D-F.** high spired gastropod shell with thickened columella and cavity filled with micrite; Whole ostracod shell with original carbonate material dissolved, leaving a mold that was replaced by microspar. Around the central ostracods are fragmented ostracod carapaces and bioclasts; Fragmented ostracod shell, bioclasts, and trilobite (Arrow) with interior filled with sparry calcite. **G-L.** phylloid algal with a fibrous wall structure interrupted by calcitic rods; transverse section of an orbitolinid foraminifera; fragmented ostracod spine surrounded by bioclasts; a well preserved impunctate brachiopod shell, bioclasts, and brachiopod spine (Arrow) with a concentric fibrous inner layer filled with micrite; biserial foraminifera with thin rims of calcite around the outer layer and inner layer filled with micrite; cross section of a cheilostome bryozoan with delicate branches. This transverse cut through the branch shows an empty zooecia. The zooecia is filled with sparry calcite and micrite.

and thick rims of calcite replacing the outer layers constitute the most abundant grain in this microfacies. They occur alongside foraminifera, serupilid worm tubes, globigerina, and pelecypods in a micrtized matrix (Figs. 6G-I).

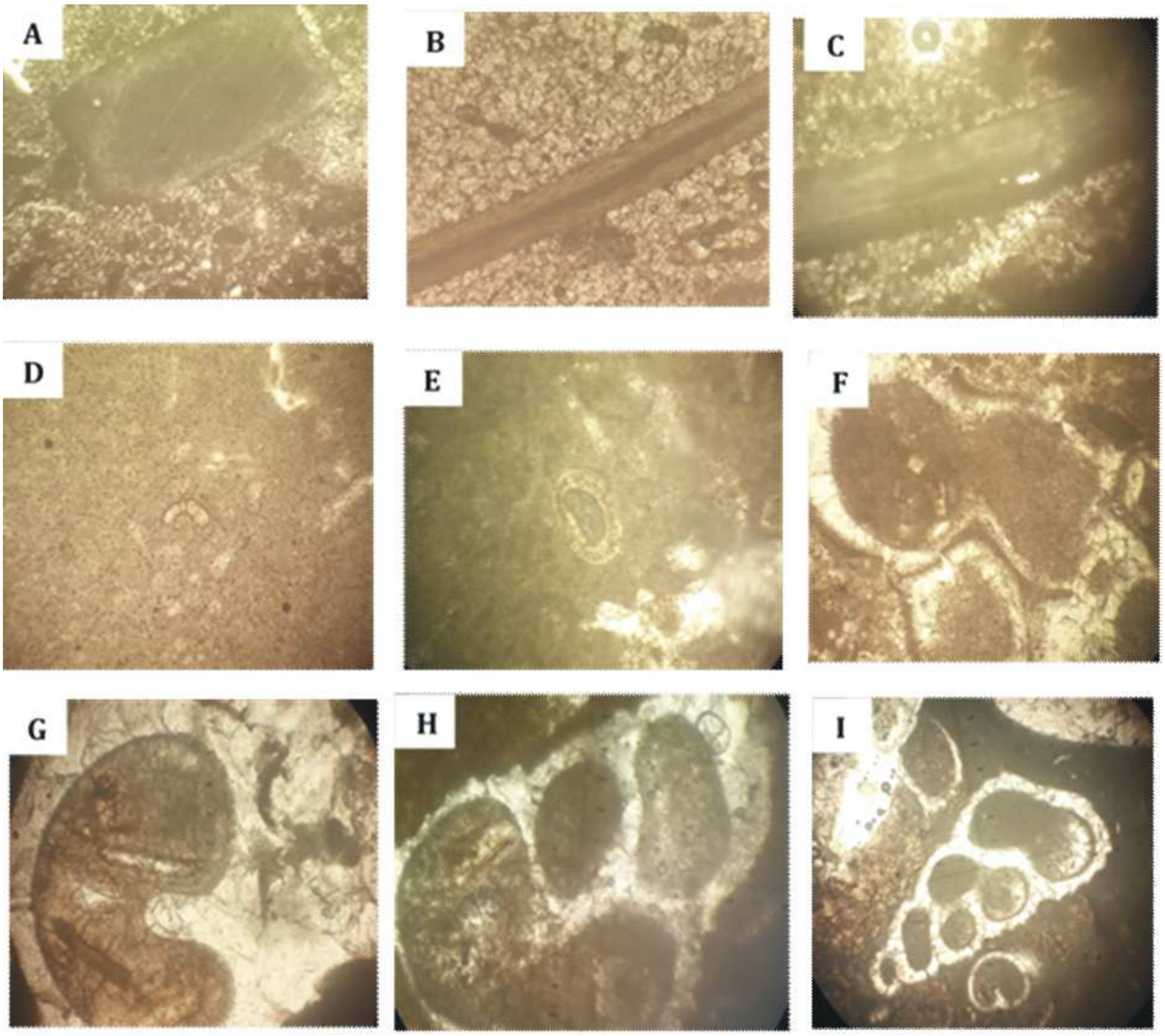

Fig. 6: A-C. an articulated crinoid columnal with a moderately varying unit extinction and a well-defined rectangular outline of the columnal; a brachiopod spine with a two-layered, fibrous wall structure and an inner layer that was obliterated by dissolution and replaced with micrite, floating on microcar cement; an impunctate brachiopod shell wall with a characteristic low-angle fibrous structure. **D-F.** fragmented differentiated test floating on mud matrix; transverse section through a brachiopod spine, with well-preserved outer layer, and micrite filled cavity, floating on micritic cement; cross section through a globigerina shell with well-preserved tests filled with calcite, and micrite filling of their chambers. **G-I.** gastropod shell with original aragonite replaced with sparry calcite and preserved by a calcite rim; gastropod shell with the internal mold replaced with microspar and rims of calcite replacing the outer layers; biserial foraminifera shell coiled tightly about its axis with outer layer preserved by thin calcite rim, underneath which there is a miniature gastropod shell.

Mineralogy

Table 1 depicts the mineralogical analytical results of the Ewekoro Limestone. The results show the dominance of calcium in all the samples. Percentage calcium content in all the samples increase down the section, whereas quartz content decreases. However, towards the base of the sections, there is increase in quartz content and decrease in calcium content. This may be attributable to the influx of terrigenous clastic materials from the continent at the early stages of limestone deposition, which later reduced as time passed by. The X-ray diffraction (XRD) results revealed higher calcite percentages in locations where thick shale overburdens are prevalent (Locations 4, 5, and 6). This is so because the overburden acts as a protective cover, shielding the underlying limestone from weathering processes such as chemical dissolution which may be caused by meteoric water infiltration. Induced pressure from overburden aids grain to grain contacts resulting in the precipitation and development of secondary minerals, such as calcite cement, which strengthens the limestone and improve its preservation.

The muscovite and albite in the studied limestone sample probably originated from the weathered crystalline rocks transported from the hinterlands.

Table 1: Mineralogical composition of outcrop samples in the study area

S/N	Calcite (%)	Quartz (%)	Muscovite (%)	Albite (%)
L1S3	61	34	4	2
L1S1	66	28	2	4
L2S3	71	7.58	14.75	6.72
L2S7	71	9	13.6	6.3
L4S1	76	15	0.9	8
L5S1	70	19	10.7	1
L5S3	76	8.9	9	6.7
L6S3	68	15.3	7.6	9
L6S6	77	15.3	0.7	7

Geochemistry

Trace Element

The concentrations of trace elements in the analyzed limestone samples are presented in table 2. These concentrations are normalized to standard trace element concentrations with Post Archean Australian Shale (PAAS) compiled by Taylor and McLennan (1985). Significant variability in transition trace elements (TTE: Co, Cr, Cu, Ni, V) and High field strength element (HFSE: Nb) and metals (Zn, and Mn) were seen in the PAAS-normalized trace element concentrations (Fig. 7). The PAAS normalized pattern of the studied limestone showed significant enrichment in Sr and depletion in Th, Nb, Cs and V.

Rare Earth Element

The concentrations of the rare earth element (REE) obtained from the analyzed limestone samples are presented in table 3. The concentrations are normalized to standard rare earth element concentrations with Post Archean Australian Shale (PAAS) compiled by Taylor and McLennan (1985). The total REE (ΣREE) of the studied limestone samples range from15.74 to 564.53 ppm (Table 3). The ΣREE contents of the studied samples are higher than the range for marine carbonates (0.04-14 ppm; Turekian and Wedepohl, 1961).

The PASS normalized REE + Y pattern of the studied limestones display relatively uniform patterns among the different litho-units (Fig. 8). Majority of the sample appeared to follow the same trend with the exception of samples L4S7 and L6S3. Sample L4S7 is the only sample that shows a distinct increment in REE concentration compared to other samples. Nevertheless, it follows a similar REE distribution pattern with other samples. Conversely, sample L6S3 is the only sample with a distinct decrease in REE concentration compared to other samples.

The limestones exhibit the following characteristics: a) an enrichment of light rare earth elements (LREEs: La-Gd) and Yttrium (Y) and a depletion of high rare earth elements (HREEs: Tb- Lu), with $(Nd/Yb)_{SN}$ ranging from 1.03 to 8.90, (SN – Shale Normalized), $(Dy/Yb)_{SN}$ ranging from 1.02 to 8.07, and low Er/Nd values ranging from 0.04 to 0.10. According to Wyndham *et al.*, (2004), these values indicate the preferential scavenging process of LREE which is the dominant process controlling the changes in the $(Nd/Yb)_{SN}$ ratio in limestones (Table 4). The high $(Nd/Yb)_{SN}$ ratio is attributable to the property of adsorption/scavenging processes in which the LREE are: a) preferentially adsorbed onto the particle surfaces and retention in solution of smaller ionic radius HREE. b) Consistent positive Ce anomaly. c) High Y/Ho ratio ranging from 26.48 to 60.0.

The bivariate plot of Pr/Pr* vs Ce/Ce* for the limestone samples from the study areas is depicted in figure 9. The plot reveals a positive Ce anomaly and a negative La anomaly.

Discussion

Microfacies Interpretation and Depositional Environment

According to Flugel (2010), an integrated approach combining different methods and using information from the sedimentary record, including microfacies analysis, is suitable for reconstructing the paleoenvironment of carbonates. The microfacies types of the studied rock samples revealed by the petrographic study of the thin sections revealed the presence of diverse fossil organisms typical of shallow warm marine environments. Two types of cement were observed in the studied samples; a primary micrite and a secondary sparry calcite formed through recrystallization of the primary carbonate material.

Table 2: PAAS Normalized Trace elements concentrations (ppm) of Limestones from the study area

SAMPLE ID	Co	Cu	Ni	V	Zn	Cr	Mn	Cs	Nb	Rb	Sr	Th	U	Pb	Mo
L1S1	0.20	0.60	0.41	0.14	0.41	0.41	0.16	0.09	0.08	0.06	122.57	0.03	1.07	5.59	2.00
L1S3	0.26	0.60	1.52	0.23	0.48	0.88	0.55	0.11	0.40	0.06	108.29	0.08	0.36	3.88	5.33
L2S1	0.15	1.20	0.32	0.05	0.48	0.41	0.31	0.07	0.12	0.04	116.57	0.06	1.07	1.18	6.00
L2S3	0.13	0.60	1.86	0.19	0.76	0.87	0.36	0.07	0.12	0.05	89.43	0.16	0.36	1.71	0.67
L2S5	0.19	1.00	0.36	0.19	0.55	0.76	0.68	0.09	0.12	0.08	96.86	0.09	0.36	1.06	4.00
L2S7	0.76	1.00	0.34	0.33	0.62	0.71	2.17	0.11	0.16	0.07	105.43	0.14	1.43	1.18	6.00
L4S1	0.23	2.20	1.57	0.19	1.17	0.94	0.26	0.07	0.12	0.05	82.29	0.09	0.36	1.59	2.00
L4S3	0.19	0.20	0.25	0.37	1.11	1.12	0.17	0.04	0.08	0.04	85.43	0.15	0.36	1.47	0.67
L4S5	0.09	1.20	1.09	0.14	0.55	0.53	0.45	0.04	0.12	0.04	116.29	0.07	0.36	0.41	4.00
L4S7	1.82	2.20	1.66	1.44	1.32	2.22	1.69	0.22	1.00	0.05	22.86	0.80	1.07	4.06	5.33
L5S1	0.15	0.20	0.48	0.14	0.69	0.82	0.26	0.07	0.12	0.04	137.71	0.09	0.71	1.24	0.67
L5S3	0.15	0.20	0.11	0.19	0.48	1.65	0.18	0.07	0.04	0.04	120.00	0.07	1.43	0.65	0.67
L5S7	0.10	0.20	1.18	0.14	0.27	0.53	0.53	0.04	0.08	0.04	103.43	0.07	1.07	1.18	0.67
L5S9	0.15	0.80	1.52	0.33	0.90	1.58	1.54	0.11	0.24	0.09	96.57	0.14	2.14	1.29	1.33
L6S1	0.15	0.20	1.25	0.33	1.18	1.65	0.19	0.07	0.08	0.04	166.86	0.15	0.71	1.12	2.00
L6S3	0.18	0.80	0.11	0.19	0.90	0.82	0.06	0.11	0.04	0.05	280.86	0.07	0.36	0.06	8.00
L655	0.20	0.20	0.86	0.14	0.76	0.82	0.09	0.09	0.08	0.05	247.43	0.14	0.71	1.24	0.67
L656	0.18	0.20	1.27	0.05	0.90	0.47	0.31	0.11	0.12	0.06	112.57	0.12	0.36	1.76	0.67
L658	0.11	3.60	0.27	0.14	4.97	0.82	0.48	0.07	0.32	0.04	113.71	0.07	0.36	0.76	3.33
L754	0.12	1.00	0.11	0.28	0.55	0.82	2.36	0.07	0.04	0.06	113.43	0.10	1.43	1.06	0.67

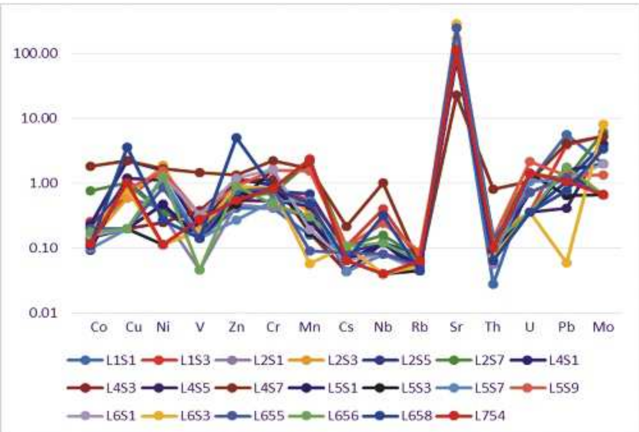

Fig. 7: PAAS-normalized trace elements distribution of limestone samples at the study area.

These cements hold information on the hydrodynamic controls (depositional water energy) under which the sediments were deposited. The presence of micrite suggests low energy environment characterized by gently moving water commonly associated with slow sediments accumulation. Whereas, sparry calcite is a diagenetic product precipitated after the deposition of calcium rich sediments. Microfacies interpretation indicate the dominance of packstone over wackstone. This suggests the prevalence of high energy over the quiet, low energy environmental condition during the accumulation of the Ewekoro Limestone.

Source of REE

The amount of REE found in sediments can be influenced by various factors, including the authigenic removal of REE from the water column and early diagenesis (Sholkovitz and Elderfield, 1988); the biogenic deposition of sediments from overlying seawater (Murphy and Dymond, 1984); input of terrigenous particles from continental sources (Liu et al., 1988); scavenging processes associated with depth, salinity, and oxygen levels (Greaves et al., 1999).

Nothdurft et al., (2004) indicated that samples with a seawater-like pattern contribute a lesser amount of REE to the chemical sediments. Conversely, samples exhibiting non-seawater-like patterns showed higher concentrations of REE. The increased REE concentration in non-seawater-like patterns can be attributed to the contamination by materials such as silicates, Fe-Mn oxides, phosphates, or sulfides during the chemical leaching process (Zhao et al., 2009). The total REE (ΣREE) content in original carbonates is expected to be low, and the presence of elevated ΣREE content can be attributed to these non-carbonate contaminants originating from hydrothermal sources and/or terrestrial particulate matter (Frimmel, 2009). In the study area, the ΣREE values of limestone samples exhibited significant variation, ranging from 15.74 to 564.53 ppm. These values surpassed the range typically observed for marine carbonates (0.04-14 ppm; Turekian and Wedepohl, 1961) as well as the average value for

Table 3: Rare earth elements concentrations (ppm) for limestones from the study area

SAMPLE ID	La	Ce	Pr	Nd	Sm	Eu	Gd	Tb	Dy	Y	Ho	Er	Tm	Yb	Lu	ΣREE
L1S1	5.5	7.6	1.16	4.8	1.1	0.18	0.96	0.1	0.67	5.2	0.13	0.34	0.025	0.05	0.025	27.84
L1S3	21.4	36	4.63	18.6	4.1	0.85	3.56	0.48	2.99	16.8	0.53	1.45	0.21	0.8	0.18	112.58
L2S1	5.6	8.1	1.21	5.2	1.3	0.18	0.98	0.12	0.92	5.9	0.17	0.46	0.05	0.1	0.025	30.315
L2S3	11.4	19.9	2.61	12.1	2.6	0.49	2.34	0.32	1.63	10.5	0.25	0.74	0.1	0.5	0.12	65.6
L2S5	7.3	11.2	1.61	7	1.3	0.31	1.34	0.16	0.95	6.5	0.19	0.46	0.06	0.3	0.08	38.76
L2S7	17.1	31.5	3.72	14.4	2.9	0.61	3.28	0.4	2.61	18.6	0.48	1.44	0.14	0.9	0.15	98.23
L4S1	16	31.3	3.92	16.2	2.9	0.61	2.32	0.3	1.82	11.1	0.34	0.89	0.1	0.6	0.11	88.51
L4S3	20.3	43.6	5.64	22.6	3.8	0.91	3.09	0.42	2.22	11	0.41	0.95	0.1	0.8	0.12	115.96
L4S5	13.7	11.6	3.68	12	2	0.45	1.81	0.21	1.14	9.4	0.31	0.86	0.025	0.4	0.025	57.61
L4S7	99.2	192	25.42	103	21.5	4.46	19.08	2.61	13.8	67	2.53	6.72	0.9	5.5	0.81	564.53
L5S1	9.5	19.1	2.47	10.2	2.1	0.34	1.69	0.2	1.23	6.8	0.23	0.46	0.06	0.5	0.06	54.94
L5S3	7.2	10.9	1.51	6.5	1	0.22	1.17	0.12	0.87	6.5	0.15	0.34	0.06	0.1	0.05	36.69
L5S7	12	19.5	2.78	11.5	2.2	0.32	1.81	0.22	1.26	8.5	0.27	0.84	0.07	0.5	0.07	61.84
L5S9	10.8	19.8	2.73	11.3	2.4	0.45	2.66	0.31	1.47	10.8	0.36	0.98	0.09	0.6	0.08	64.83
L6S1	13.7	29.3	3.58	15.2	2.6	0.54	2.5	0.26	1.43	7.5	0.22	0.56	0.09	0.4	0.07	77.95
L6S3	3.6	6.1	0.71	2.5	0.5	0.025	0.28	0.025	0.17	1.5	0.025	0.15	0.025	0.1	0.025	15.735
L6S5	10.6	20.7	2.57	10.7	1.7	0.42	1.31	0.18	0.86	5.3	0.13	0.4	0.025	0.1	0.05	55.045
L6S6	15.5	28.7	4.03	15.7	3.1	0.55	2.6	0.35	1.65	9.4	0.28	0.71	0.08	0.5	0.025	83.175
L6S8	4	6.4	0.87	3.7	1	0.19	0.81	0.1	0.54	4.3	0.13	0.36	0.025	0.3	0.025	22.75
L7S4	7.4	12.7	1.73	6.6	1.3	0.34	1.36	0.15	0.97	6.8	0.16	0.6	0.06	0.3	0.06	40.53

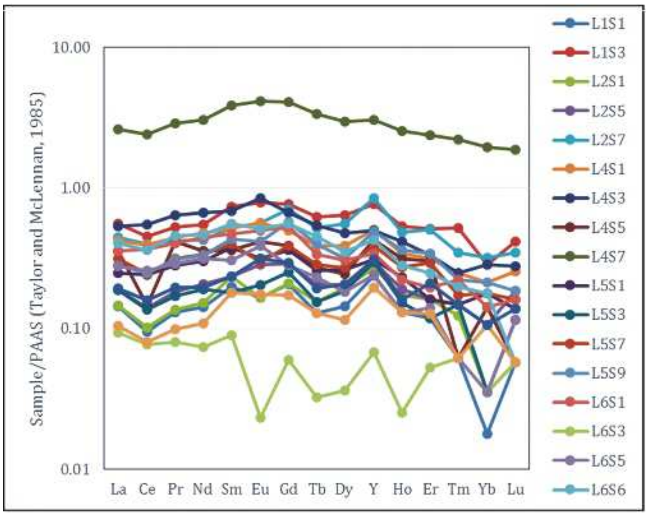

Fig. 8: PAAS-normalized rare earth elements distribution of limestone samples from the study area.

Table 4: Range of element ratios of the limestone from the study area compared to felsic and mafic rocks of UCC and PASS

Elemental Ratio	Ewekoro Formation[1]		Range of Sediments[2]		UCC[3]	PASS[3]
	Min	*Max*	*Felsic*	*Mafic Rocks*		
Eu/Eu*	0.31	1.33	0.40-0.94	0.71-0.95	0.63	0.66
La/Co	1.16	8.56	1.80-13.8	0.14-0.38	1.76	1.65
Th/Co	0.09	0.77	0.67-19.4	0.04-1.40	0.63	0.63
Th/Cr	0.01	0.05	0.13-2.7	0.018-0.046	0.13	0.13
Cr/Th	21.98	200	4.00-15.0	25-500	7.76	7.53

[1]Present study, n = 20
[2]Cullers (1994, 2000); Cullers and Podkovyrov (2000); Cullers *et al.* (1988)
[3]Taylor and McLennan (1985).

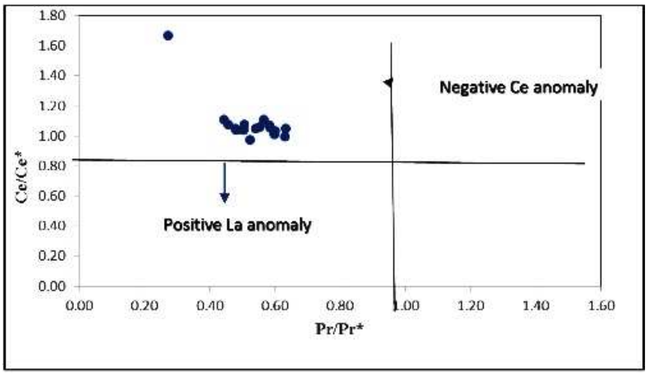

Fig. 9: Plot of PAAS-normalized Pr/Pr* vs Ce/Ce* (modified after Bau and Dulksi, 1996)

typical marine carbonates (~28 ppm; Bellanca et al., 1997).

The Er/Nd ratio serves as an indicator of LREE/HREE fractionation in modern and ancient marine systems, as discussed by German and Elderfield (1989). Normal seawater exhibits an Er/Nd ratio of approximately 0.27 (De Baar et al., 1988). Elevated Er/Nd ratios indicate the presence of a seawater signature preserved in the marine carbonates. However, the addition of detrital material or diagenetic processes can reduce the Er/Nd value to less than 0.1 due to preferential concentration of Nd relative to Er (Bellanca et al., 1997). The studied limestones displayed Er/Nd ratios ranging from 0.04 to 0.10, with an average of 0.07, suggesting the influence of detrital sources on REE concentrations. The negative and weak correlations observed between ΣREE content and diagenetic proxies further support the presence of detrital contaminants in the studied limestones. The weak negative correlation between ΣREE and Sr (r = -0.49) indicates that the influence of diagenetic processes on REE concentrations is limited.

The application of La/Co, Th/Co, Th/Cr, and Cr/Th ratios is widely employed in the investigation of source region composition, which is shown by variation in these ratios based on the contribution from felsic and mafic (Armstrong-Altrin, 2009). In the present study, the La/Co, Th/Co, Th/Cr, and Cr/Th ratios of the analyzed limestone samples were compared with those of felsic and mafic rocks (fine fraction), as well as with the average upper continental crust (UCC) and PAAS values (Table 3). The results indicate that these ratios fall within the range of intermediate to felsic rocks.

Y/Ho Ratio

Yttrium occupies a position between Ho and Dy in the REE +Y pattern due to its similar charge and comparable atomic radius (Bau, 1996). Unlike its geochemical counterpart Ho, Y remains in seawater due to differences in surface complex stability, resulting in a notably super chondritic marine Y/Ho ratio (Bau, 1996). In general, seawater exhibits high Y/Ho ratios (~44-74), while terrigenous materials and volcanic ash maintain consistent chondritic Y/Ho ratios (~28). The analyzed limestone samples demonstrate variation in Y/Ho ratios ranging from 26.48 to 60.0, with an average of 35.8. Most of the samples exhibit Y/Ho ratios higher than the chondritic value (~28) but lower than the super chondritic value observed in seawater. The observed variation in Y/Ho ratios in this study suggests that the limestones of the Ewekoro Formation is contaminated by terrigenous materials.

Cerium Anomaly (Ce/Ce*)

The Ce anomaly is a useful tool for interpreting the redox conditions in seawater during the incorporation of rare earth elements (REE) into marine sediments (Madhavaraju and Lee, 2009). Unlike other REEs, Ce has the potential to be oxidized in seawater, transitioning from the Ce^{3+} to the less soluble Ce^{4+} oxidation state (Nagendra et al., 2011). In well-oxygenated seawater, the Ce^{4+} can be incorporated into marine sediments, leading to an enrichment of Ce in the sediment relative to other REEs (Bellanca et al., 1997). This process of Ce enrichment in sediments results in a depletion of Ce in seawater compared to other rare earth elements (Bellanca et al., 1997). The Ce/Ce* values observed in the limestone samples from the study area range from 0.27 to 0.63, with an average of 0.54 ± 0.08 (n=20). All the analyzed samples exhibit Ce/Ce* values below 1. In seawater, Ce/Ce* values typically range from 0.1 to 0.4 (Elderfield and Greaves, 1982; Piepgras and Jacobsen, 1992), while the average shale value is 1 (Cullers and Stone, 1991). This suggests that the Ce/Ce* values in the limestone samples from the study area have been influenced by the precipitation processes involving seawater.

Under suboxic conditions, Ce can be mobilized and released into the water column, resulting in a positive anomaly in seawater (De Baar, 1991). Furthermore, the interpretation of Ce anomalies from Ce/Ce* values can be complicated by the variable La content. Enrichment of La can occasionally lead to an overstatement of negative Ce anomalies (Bau and Dulski, 1996). To address these complexities, the Pr/Pr* vs Ce/Ce* discriminant diagram (Fig. 9), initially proposed by Bau and Dulski (1996) and modified by Webb and Kamber (2000), allows for the assessment of "true" Ce anomalies and the extent of La enrichment. Positive Ce anomaly majorly occur due to detrital inputs (Madhavaraju and Lee 2009) scavenging process (Masuzawa and Koyama, 1989), diagenesis (Armstrong-Altrin et al., 2003), and anoxic condition (German and Elderfield, 1990).

Paleo-Oxygenation Conditions

Redox-sensitive trace elements exhibit greater solubility in oxidizing environments compared to reducing environments, leading to their enrichment in authigenic minerals within anoxic deposition settings (Zuo et al., 2020). This characteristic establishes elements such as U, V, Mo, Cr, and others as valuable indicators for assessing the redox properties of aquatic systems. Furthermore, certain elements that are sensitive to redox conditions, including Ni, Cu, Zn, and Cd, are absorbed by organic matter and subsequently incorporated into sediments, thereby serving as indicators of a reducing environment (Sial et al., 2015; Yang et al., 2018). The ratios of redox-sensitive trace elements have been employed to interpret the prevailing depositional environment (Abou El-Anwar et al., 2019; Jeon et al., 2020). Consequently, parameters such as V/(V + Ni), V/Ni, and V/Mo can be used to determine the redox conditions within a given depositional environment.

A V/Ni ratio greater than 3 signifies the deposition of organic matter under reducing marine environments (Galarraga et al., 2008). V/Ni ratios ranging from 1.9 to 3 suggest deposition under dysoxic to oxic environments, with a mixture of terrigenous and marine organic matter. V/Ni ratios below 1.9 indicate the deposition of terrigenous organic matter under oxic conditions. The V/Ni ratios of the studied samples vary from 0.09 to 6.00 with an average of 1.48, suggesting that the samples were deposited under varying suboxic to oxic conditions.

According to Jeon et al. (2020), a higher V/ (V + Ni) value indicates a more strongly reducing condition compared to anoxic conditions. A V/ (V + Ni) value greater than 0.60 suggests an anoxic depositional environment, while values between 0.46 and 0.60 indicate a suboxic environment, and values below 0.46 indicate an oxic depositional environment. The V/ (V + Ni) values observed in the limestone samples analyzed in this study ranged from 0.08 to 0.86, suggesting that they are deposited under suboxic to anoxic conditions.

The V/Mo ratio of <2, indicates an anoxic condition, a range from 2 to 10 indicates suboxic condition and a range from 10 to 60 indicates normal oxygenation (Abou El-Anwar et al. 2019). The V/Mo ratio of the studied limestone samples ranges from 0.58 to 19.25, indicating that they were deposited under anoxic to suboxic conditions.

The Th/U ratio can be used as indicator for redox conditions. Uranium, being a redox-sensitive element, maintains a predominantly higher oxidation state, U6+ in oxidizing environments, resulting in the formation of a water-soluble uranyl carbonate compound. Conversely, under reducing conditions, uranium retains a lower oxidation state, U4+, leading to the formation of an insoluble uranium fluoride compound that becomes trapped within marine carbonates (Wignall and Twitchett 1996). In contrast, Thorium is not influenced by the redox conditions within the water column and consequently persists in the insoluble Th4+ state. This disparity indicates that sediments situated in anoxic environments exhibit higher uranium content and lower Th/U ratios compared to those in oxygenated environments. The Th/U ratios have been employed as a means to ascertain the redox conditions of the environment, with ratios less than 2 signifying anoxic marine sediments, ratios ranging from 2 to 7 indicating oxic sediments, and ratios exceeding 7 suggesting highly oxygenated terrestrial environments. In the present study, analysis of limestone samples revealed Th/U ratios ranging from 0.1 to 2.87, with an average value of 0.81. Furthermore, an overwhelming majority of the analyzed samples (over 95%) exhibited ratios below 2, providing evidence of limestone precipitation occurring in anoxic to dysoxic conditions.

Conclusions

The petrography study indicated the deposition of the limestone in a fluctuating low energy to high energy environments. The presence of micrite suggested a low energy environment while calcite cements suggested a high energy environment. In addition, the microfacies types, indicated that the limestones were deposited in the close lagoonal, open lagoonal, and restricted shoal environments.

The geochemical analysis showed a variation in elemental concentrations. Trace element ratios of V/Mo, V/ (V/Ni), and Th/U suggested that the limestones were deposited under oxic to anoxic conditions. The average V/Ni ratio indicated terrigenous material contribution to the marine environment, probably resulting from runoff from rivers emptying their contents into the coastal areas. The enrichment of LREE and the depletion of HREE in the limestone suggests the retention of non-seawater patterns. The REE signatures, such as the low Er/Nd, and the varied Y/Ho ratios, indicates that the REE concentration of the limestone was mainly influenced by terrigenous (detrital) contamination. The positive Ce anomaly and the varied Mn* value suggests that the limestones were deposited under varying suboxic to oxic conditions.

References

Abou El-Anwar, E.A., Mekky, H.S., Salman, S. A. Elnazer, A. A., Abdel Wahab, W., and Asmoay, A. S. (2019). Mineralogical and petrographical studies of agricultural soil, Assiut Governorate, Egypt. Bulletin of the National Research Centre, doi.org/10.1186/s42269-019-0068-z

Adekeye, O.A. and Akande, S.O. (2006). Depositional Environment and the reservoir Potential Assessment of the Paleocene Ewekoro Formation, Eastern Dahomey Basin, Southwestern Nigeria. Journal of Mining and Geology, 42(1), pp. 133-140.

Akaegbobi, I. M. and Ogungbesan, G. O. (2016). Geochemistry of the Paleocene Limestones of Ewekoro Formation, Eastern Dahomey Basin, Southwestern Nigeria. Implication on

Provenance and Depositional Conditions. Ife Journal of Science, 18(3), pp. 669-684.

Alonso-Zarza, A.M. (2003). Paleoenvironmental significance of palustrine carbonates and calcretes in the geological record. Earth Sci. Rev. 60, pp, 261–298.

Armstrong-Altrin, J.S., Verma, S.P., Madhavaraju, J., Lee, Y.I., and Ramasamy, S. (2003). Geochemistry of Late Miocene Kudankulam Limestones, South India. International Geology Review, 45, pp. 16–26.

Armstrong-Altrin, J.S. (2009). Provenance of sands from Cazones, Acapulco, and Bahía Kino beaches, Mexico. Revista Mexicana de Ciencias Geológicas, 26 (3), pp. 764-782.

Bankole, S. I., Opatola, A. O., Akinmosin, A., Omeru, T., Ezenwobi, N. H. and Oti, M. N. (2021). Diagenetic Study of the Paleocene Ewekoro Limestone, Dahomey (Benin) Basin, Nigeria. Ekiti State University Journal of Science and Technology (EJST), 6 (1&2), pp. 75-87.

Bankole, S. I., Schrank, E., Erdtmann, B. D and Akande, S. O. (2006). Palynostratigraphic Age and Paleoenvironments of the newly exposed section of the Oshoshun Formation in the Sagamu Quarry, Dahomey Basin. Nigerian Association of Petroleum Explorationists Bulletin, 19(1), pp. 25-34.

Bau, M. (1996). Controls on the fractionation of isovalent trace elements in magmatic and aqueous systems: Evidence from Y/Ho, Zr/Hf, and lanthanide tetrad effect. Contributions to Mineralogy and Petrology, 123, pp. 323-333.

Bau, M. and Dulski, P. (1996). Anthropogenic origin of positive gadolinium anomalies in river waters. Earth and Planetary Science Letters, 143, pp. 245-255.

Bellanca, A., Masetti, D., and Neri, R. (1997). Rare earth elements in limestone/marlstone couplets from the Albian-Cenomanian Cismon section (Venetian region, northern Italy): assessing REE sensitivity to environmental changes. Chemical Geology, 141, pp. 141-152.

Bertram, C J, and Elderfield, H. (1993). The geochemical balance of the rare earth elements and neodymium isotopes in the oceans. Geochimica et Cosmochimica Acta, 57(9), pp. 0016-7037.

Billman, H.G. (1976). Offshore stratigraphy and paleontology of Dahomey Embayment. Proc.7th Afri, Micropal, Coll. Ile-Ife, pp. 27-42.

Cullers, R.L. (1994). The controls on the major and trace element variation of shales, siltstones and sandstones of Pennsylvanian – Permian age from uplifted continental blocks in Colorado to platform sediment in Kansas, USA. Geochimica et Cosmochimica Acta, 58(22), pp. 4955-4972.

Cullers, R.L. (2000). The geochemistry of shales, siltstones and sandstones of Pennsylvanian Permian age, Colorado, U.S.A.: implications for provenance and metamorphic studies. Lithos, 51, pp. 305-327.

Cullers, R.L., Basu, A., and Suttner, L. (1988). Geochemical signature of provenance in sand-size material in soils and stream sediments near the Tobacco Root batholith, Montana, USA. Chemical Geology, 70(4): 335-348.

Cullers, R.L., and Stone, J. (1991). Chemical and mineralogical composition of the Pennsylvanian Mountain, Colorado, U.S.A. (an uplifted continental block) to sedimentary rocks from other tectonics environments. Lithos, 27, pp. 115-131.

Cullers, R.L., and Podkovyrov, V.N. (2000). Geochemistry of the Mesoproterozoic Lakhanda Shales in southeastern Yakutia, Russia: implications for mineralogical and provenance control, and recycling. Precambrian Research, 104(1-2), pp. 77-93.

De Baar, H.J.W. (1991). On cerium anomalies in the Sargasso Sea. Geochimica et Cosmochimica Acta, 55, pp. 2981-2983.

De Baar, H.J.W., German, C.R., Elderfield, H., and Van Gaans, P. (1988). Rare earth element distributions in anoxic waters of the Cariaco Trench. Geochimica et Cosmochimica Acta, 52, pp. 1203-1219.

Dunham, R.J. (1962). Classification of carbonate rocks according to depositional texture, in Ham, W. E., ed., Classification of Carbonate Rocks: AAPG Memoir, 1, pp. 108–121.

Elderfield, H., and Greaves, M.J. (1982). The rare earth elements in seawater. Nature, 296, pp. 214-219.

Flugel, E. (2010). Microfacies of Carbonate Rocks, Analysis, Interpretation and Application. Springer-Verlag, Berlin, p. 976.

Frimmel, H.E. (2009). Trace element distribution in Neoproterozoic carbonates as paleoenvironmental indicator. Chemical Geology, 258, pp. 338-353.

Galarraga, F., Reategui, K., Martïnez, A., Martínez, M., Llamas, J.F., Márquez, G. (2008). V/Ni ratio as a parameter in palaeoenvironmental characterisation of nonmature medium-crude oils from several Latin American basins. Journal of Petroleum Science and Engineering, 61(1), pp. 9-14.

German, C.R., and Elderfield, H. (1989). Rare earth elements in Saanich Inlet, British Columbia, a seasonally anoxic basin. Geochimica et Cosmochimica Acta, 53, pp. 2561-2571.

German, C.R., and Elderfield, H. (1990). Application of the Ce anomaly as a paleoredox indicator: the ground rules. Paleoceanography, 5, pp. 823–833.

Greaves, M.J., Elderfield, H., and Sholkovitz E. R. (1999). Aeolian sources of rare earth elements to the Western Pacific Ocean. Marine Chemistry, 68, pp. 31-38.

Jeon, J., Shin. D., and Im, H. (2020). Depositional environment of redox sensitive trace elements in the Metalliferous Black Slates of the Okcheon Metamorphic Belt, South Korea. Geosci J, 24(2), pp. 177–19.

Jones, H.A and Hockey, R.D. (1964). Geology of parts of Southwestern Nigeria. Nigeria Bull. Geol., 31.

Kerr, A.C. (2014). Oceanic plateaus. In: Holland, H.D., Turekian, K.K. (Eds.), Treatise on Geochemistry, second ed.. Elsevier, Oxford, 4, pp. 631-667.

Liu, Y.G., Miah, M.R.U., and Schmitt, R.A. (1988). Cerium: a chemical tracer for paleo-oceanic redox conditions. Geochimica et Cosmochimica Acta, 52, pp. 1361-1371.

Madhavaraju, J., and Lee I.I. (2009). Geochemistry of the Dalmiapuram Formation of the Uttatur Group (Early Cretaceous), Cauvery Basin, Southeastern India: Implications on Provenance and Paleo-Redox Conditions. Revista Mexicana de Ciencias, 26, pp. 380-394.

Madhavaraju, J., and Ramasamy, S. (1999). Rare Earth Elements in Limestones of Kallankurichchi Formation of Ariyalur Group, Tiruchirapalli Cretaceous, Tamil Nadu. Journal of the Geological Society of India, 54, pp. 291-301.

Masuzawa, T., and Koyama, M. (1989). Settling particles with positive Ce anomalies from the Japan Sea. Geophysical Research Letters, 16, pp. 503-506.

Murphy, K., and Dymond, J. (1984). Rare earth element fluxes and geochemical budget in the eastern equatorial Pacific. Nature, 307, pp. 444-447.

Murray, R.W., Buchholtz Brink, M.R., Brink, M.R., Gerlach, D.C., Russ III, G.P., and Jones, D.L. (1991). Rare earth, major and trace elements in chert from the Franciscan complex and Monterey group, California: assessing REE sources to fine grained marine sediments. Geochimica et Cosmochimica Acta, 55, pp. 1875–1895.

Nagendra, R., Nagarajan, R., Bakkiaraj, D., and Armstrong-Altrin, J.S. (2011). Depositional and post-depositional setting of maastrichtian limestone, ariyalur Group, cauvery basin, south India: a geochemical appraisal. Carbonates Evaporites, 26, pp. 127-147.

Nath, B.N., Bau, M., Ramalingeswara Rao, B. and Rao, C.M. (1997). Elemental variation in Arabian Sea sediments through a trans minimum zone. Geochimica et Cosmochimica Acta, 61, pp. 2375–2388.

Nothdurft, L., Webb, G.E., and Kamber, B.S. (2004). Rare Earth Element Geochemistry of Late Devonian Reefal Carbonates, Canning Basin, Western Australia: Confirmation of a Seawater REE Proxy in Ancient Limestones. Geochimica et Cosmochimica Acta, 68, pp. 263-283.

Ogbe, F.G.A. (1972). Stratigraphy of Strata exposed in Ewekoro quarry, Western Nigeria. In: T.F.J. Dessauvagie and A.J. Whiteman (eds.): African Geology, Ibadan University Press, Ibadan. pp. 305–322.

Omatsola, M.E., and Adegoke, O.S. (1981). Tectonic evolution and Cretaceous stratigraphy of the Dahomey Basin. Journal of Mining and Geology, 18(1), pp. 130-137.

Piepgras, D.J. and Jacobsen, S.B. (1992). The behaviour of rare earth elements in seawater: Precise determination of ferromanganese crusts. Geochimica et Cosmochimica Acta, 56, pp. 1851-1862.

Reyment, R.I. (1965). Aspects of the Geology of Nigeria. Ibadan University Press, Ibadan. 27.

Sholkovitz, E. R., and Elderfield, H. (1988). Cycling of dissolved rare earth elements in Chesapeake Bay. Global Biogeochemical Cycles, 2(2), pp. 157-176.

Sial, A.N., Gaucher, C., and Ferreira, V.P. (2015). Isotope and elemental chemostratigraphy. Chemostratigraphy – Concepts, Techniques, and Applications, 32, pp. 23–64.

Siby, K., Nath, B.N., Ramaswamy, V., Naman, D., Gnaneshwar Rao, T., Kamesh Raju, K.A., Selvaraj, K. and Chen, C.T.A. (2008). Possible detrital, diagenetic and hydrothermal sources for Holocene sediments of the Andaman backarc basin. Mar Geol., 247, pp. 178–193.

Taylor, S.R., and McLennan, S.M. (1985). The Continental Crust: its Composition and Evolution. Blackwell Scientific Publications, Oxford, p. 312.

Turekian, K.K., Wedepohl, H. (1961). Distribution of elements in some major units of the Earth's Crust. Geol Soc Am Bull, 72, pp. 175–192

Wilson, J.L. (1975). Carbonate Facies in Geological History. Springer Verlag.

Webb, G.E., and Kamber, B.S. (2000). Rare Earth Elements in Holocene Reefal Microbialites: A New Shallow Seawater Proxy. Geochimica et Cosmochimica Acta, 64, pp. 1557-1565.

Wyndham, T., Mcculloch, M., Fallon, S., and Alibert, C. (2004). High-resolution coral records of rare earth elements in coastal seawater: Biogeochemical cycling and a new environmental proxy. Geochimica et Cosmochimica Acta, 68(9), pp. 2067–2080.

Wignall, P.B., and Twitchett, R.J. (1996). Oceanic Anoxia and the End Permian Mass Extinction. Science, 272, pp. 1155-1158.

Yang, T., Cao, Y.C., and Friss, H. (2018). Diagenetic evolution and chemical changes of deep-water mudstones of Shahejie formation in the Dongying sag, Jiyang depression, eastern China. Marine and Petroleum Geology, 93, pp. 14–31.

Zhang, K.J., Xia, B., Zhang, Y.X., Liu, W.L., Zeng, L., Li, J.F. and Xu, L.F. (2014). Central Tibetan Meso-Tethyan oceanic plateau. Lithos, pp. 210–288.

Zhao, Y.Y., Zheng, Y.F., and Chen, F. (2009). Trace element and strontium isotope constraints on sedimentary environment of Ediacaran carbonates in southern Anhui, South China. Chemical Geology 265, pp. 345-362.

Zuo, X., Li, C., Zhang, J., Ma, G., Chen, P. (2020). Geochemical characteristics and depositional environment of the Shahejie Formation in the Binnan Oilfield, China. Journal of Geophysics and Engineering, 17 (3), pp. 539-551.